ORIGINAL RESEARCH

Activation of Anoctamin-1 Limits Pulmonary Endothelial Cell Proliferation via p38–Mitogen-activated Protein Kinase–Dependent Apoptosis

Ayed M. Allawzi[1,2], Alexander Vang[1], Richard T. Clements[1,3], Bong Sook Jhun[4], Nouaying R. Kue[1], Thomas J. Mancini[1], Amy K. Landi[4], Dmitry Terentyev[4], Jin O-Uchi[4], Suzy A. Comhair[5], Serpil C. Erzurum[5], and Gaurav Choudhary[1,6]

[1]Vascular Research Laboratory, Providence Veterans Affairs Medical Center, Providence, Rhode Island; [2]Department of Molecular Pharmacology, Physiology, and Biotechnology, Brown University, Providence, Rhode Island; [3]Department of Surgery and [4]Department of Medicine, Cardiovascular Research Center, Rhode Island Hospital and Alpert Medical School of Brown University, Providence, Rhode Island; [5]Lerner Research Institute, Cleveland Clinic, Cleveland Ohio; and [6]Department of Medicine, Warren Alpert Medical School of Brown University, Providence, Rhode Island

Abstract

Hyperproliferative endothelial cells (ECs) play an important role in the pathogenesis of pulmonary arterial hypertension (PAH). Anoctamin (Ano)-1, a calcium-activated chloride channel, can regulate cell proliferation and cell cycle in multiple cell types. However, the expression and function of Ano1 in the pulmonary endothelium is unknown. We examined whether Ano1 was expressed in pulmonary ECs and if altering Ano1 activity would affect EC survival. Expression and localization of Ano1 in rat lung microvascular ECs (RLMVECs) was assessed using immunoblot, immunofluorescence, and subcellular fractionation. Cell counts, flow cytometry, and caspase-3 activity were used to assess changes in cell number and apoptosis in response to the small molecule Ano1 activator, Eact. Changes in mitochondrial membrane potential and mitochondrial reactive oxygen species (mtROS) were assessed using 5,5′,6,6′-tetrachloro-1,1′,3,3′-tetraethylbenzimidazolylcarbocyanine, iodide (mitochondrial membrane potential dye) and mitochondrial

ROS dye, respectively. Ano1 is expressed in RLMVECs and is enriched in the mitochondria. Activation of Ano1 with Eact reduced RLMVEC counts through increased apoptosis. Ano1 knockdown blocked the effects of Eact. Ano1 activation increased mtROS, reduced mitochondrial membrane potential, increased p38 phosphorylation, and induced release of apoptosis-inducing factor. mtROS inhibition attenuated Eact-mediated p38 phosphorylation. Pulmonary artery ECs isolated from patients with idiopathic PAH (IPAH) had higher expression of Ano1 and increased cell counts compared with control subjects. Eact treatment reduced cell counts in IPAH cells, which was associated with increased apoptosis. In summary, Ano1 is expressed in lung EC mitochondria. Activation of Ano1 promotes apoptosis of pulmonary ECs and human IPAH-pulmonary artery ECs, likely via increased mtROS and p38 phosphorylation, leading to apoptosis.

Keywords: pulmonary arterial hypertension; endothelium; anoctamin-1; mitochondria; apoptosis

Clinical Relevance

In this article, we report, for the first time, that anoctamin (Ano)-1, a calcium-activated chloride channel, is expressed in pulmonary endothelial cell mitochondria and activation of Ano1 results in apoptosis of hyperproliferative endothelial cells. These data suggest that Ano1 can serve as a new therapeutic target in pulmonary arterial hypertension associated with plexiform arteriopathy due to hyperproliferative endothelial cells.

Pulmonary arterial hypertension (PAH) is a progressive hemodynamic disease associated with extensive remodeling of the pulmonary vasculature, resulting in increased pulmonary vascular resistance (1). The vascular remodeling in PAH is mediated in part by proliferation of pulmonary endothelial cells (ECs) (1). Specifically, dysregulated EC proliferation is a distinctive feature of PAH, resulting in the formation of plexiform lesions that occlude the lumen of vessels (2–4). In addition, pulmonary artery ECs (PAECs) isolated from patients with idiopathic PAH (IPAH; IPAH-PAECs) proliferate more than those isolated from control patients (5, 6).

Anoctamin (Ano)-1 was confirmed as the gene encoding the calcium-activated chloride channel (CaCC) in 2008 (7–9). Several studies have associated Ano1 with increased proliferation of cancer cell lines (10). In contrast, increased expression of Ano1 is associated with reduced proliferation by increasing cell cycle arrest in vascular smooth muscle cells (11). Hence, the role of Ano1 in cell proliferation and cell death is cell type specific, and is unknown in pulmonary ECs.

In this study, we determined whether Ano1 was expressed in pulmonary ECs and the effect of Ano1 activation on rat lung microvascular ECs (RLMVECs) and hyperproliferative PAECs isolated from patients with IPAH.

Methods

Please *see* the data supplement for expanded METHODS and supplemental figures.
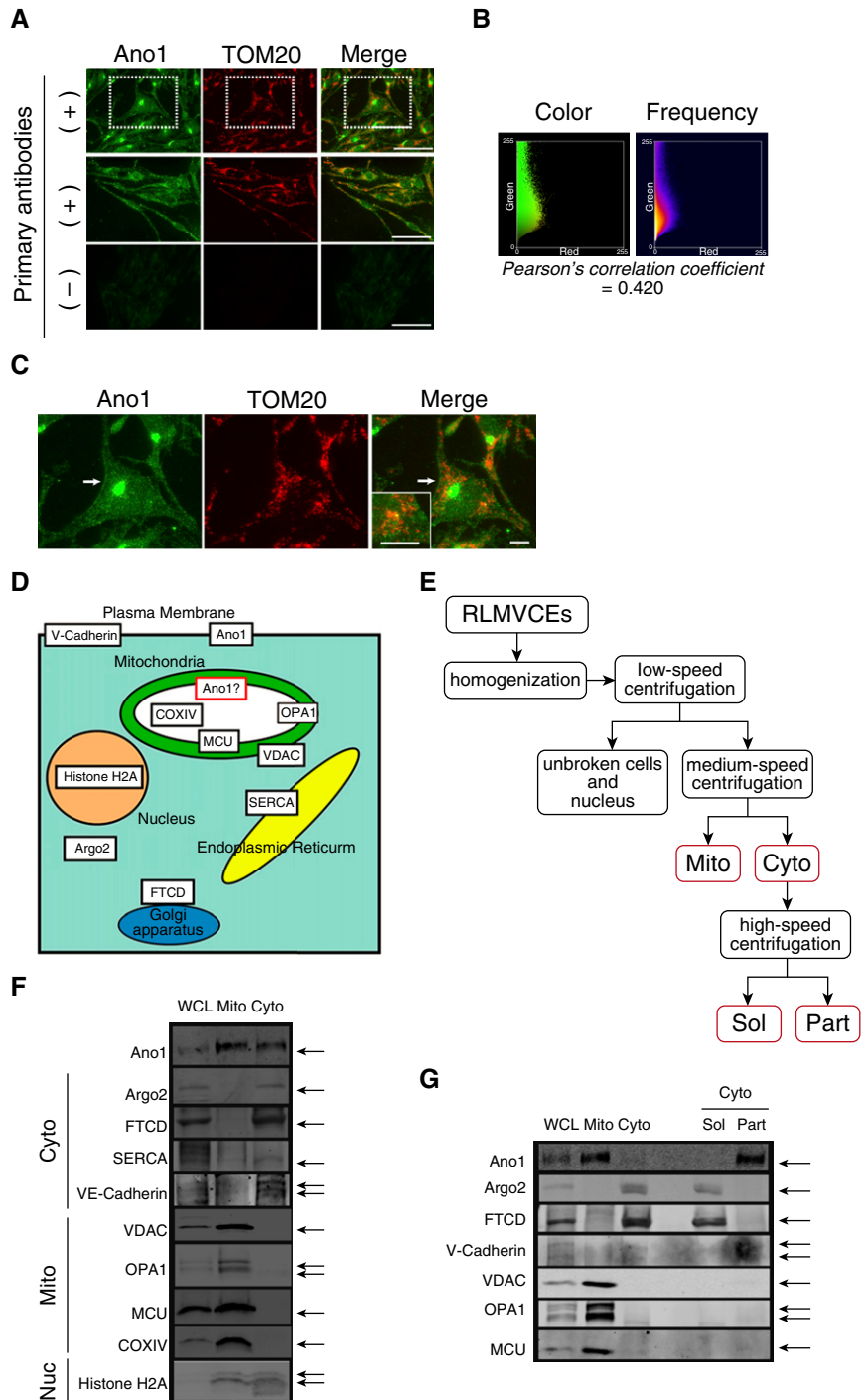
Figure 1. Subcellular localization of anoctamin (Ano)-1 in primary pulmonary endothelial cells (ECs). (*A*) Immunofluorescence images of rat lung microvascular ECs (RLMVECs) labeled with Ano1 (green) and the mitochondrial marker translocase of the outer mitochondrial membrane 20 (TOM20; red) antibodies (top and middle panels). Control experiments were performed using secondary antibodies without primary antibodies, which showed no noticeable labeling (bottom panels). Higher magnification of dotted square regions is shown in C. Scale bars = 50 μm. (*B*) Frequency and color scatter plots generated from top panel images in *A*. Pearson's correlation coefficient value calculated from *A* indicates partial colocalization of Ano1 and TOM20. (*C*) Higher magnification of RLMVEC image from *A*. Ano1 is localized to the plasma membrane (white arrow) and intracellular compartments, including mitochondria (inset). *See also* Figure E1 and Video E1. Scale bars = 10 μm. (*D*) Schematic diagram of selected marker proteins and potential subcellular Ano1 localization.

Cell Culture

RLMVECs and complete MCDB-131 media were purchased from Vec Technologies. Basal MCDB-131 was obtained from Gibco. For human PAECs, fibronectin was purchased from EMD Millipore. Endothelial cell growth medium-2 (EGM-2) and endothelial growth basal medium-2 (EBM-2) media were obtained from Lonza.

For all experiments conducted with RLMVECs, cultureware was coated with 0.2% gelatin for 30 minutes at 37°C. Media use was reserved to either complete MCDB-131 media or serum reduced MCDB-131, which was made by combining 1/10 complete MCDB-131 and 9/10 serum-free MCDB-131. Cells were quiesced with reduced serum for 24 hours. For all experiments, passages were kept between passages 4–7.

IPAH-PAECs were obtained from explanted patients diagnosed with IPAH, whereas control ECs were obtained from donor lungs not used for transplantation. The PAECs were extensively characterized, as previously described, where purity was assessed using morphometric analysis (phase–contrast along with electron microscopy), phenotypic expression of endothelial markers (endothelial nitric oxide synthase [eNOS], CD31, and Von Willebrand factor [vWF]), along with functional assays (low density lipoprotein [LDL] uptake) (12). Collection and sharing of human PAECs was approved by the Cleveland Clinic Institutional Review Board and adhered to all required ethical standards for human subject research.

In all experiments conducted using control or IPAH-PAECs, cultureware was coated with fibronectin (1 $\mu g/cm^2$) at 37°C for 1 hour. Media used with the cells were either complete EGM-2 media or serum-reduced media that were made by combining 1/25 complete EGM-2 media with 24/25 EBM-2 media. Cells were quiesced in serum-reduced conditions overnight.

Hypoxia Cell Culture

For experiments involving hypoxia exposure, cells were placed in a humidified 1% F_{IO_2}/5% CO_2 incubator (Xvivo Model G300C; Biospherix) for the indicated time; cells exposed to normoxia were placed into room-air incubators with 5% CO_2. Media were allowed to equilibrate in 1% F_{IO_2}/5% CO_2 before being added to cells, when media were changed every 2 days. Hypoxia-exposed cells were collected in a hypoxic environment.

Statistical Analysis

Unpaired two-tailed Student's t test (one-, two-, or three-way ANOVA) was used when indicated, followed by Tukey's *post hoc* pairwise comparison to determine significant differences between means. A P value less than 0.05 was considered statistically significant. Data are expressed as mean ($\pm$SEM) unless otherwise indicated.

Results

Ano1 Is Expressed in Pulmonary Endothelial Cells and Exists in the Mitochondria

Subcellular localization of Ano1 was first determined by coimmunostaining of Ano1 and a mitochondria-specific protein, the translocase of the outer mitochondrial membrane 20 (TOM20) in RLMVECs. Immunofluorescent images showed both intracellular punctate and plasma membrane staining (Figures 1A–1C; *see also* Figure E1 and Video E1 in the data supplement). Small-size intracellular dots were partially colocalized with TOM20 with a Person's correlation coefficient value (13, 14) of 0.49 ($\pm$0.02; $n = 31$) (*see also* the supplementary METHODS in the data supplement), whereas large and strong fluorescent spots at the cytosol were localized with the Golgi system, confirmed by costaining with a Golgi 58 K protein,

formimino-transferase cyclodeaminase (FTCD), an enzyme associated with the cytoplasmic surface of the Golgi apparatus (15) (Figure 1D and Figure E2). To further examine the subcellular localization of Ano1, mitochondria-enriched (Mito) fraction as well as cytosolic (Cyto) fraction containing other cellular organelles were prepared from RLMVECs (Figure 1E). Purity as well as the structural integrity of isolated mitochondria in the Mito fraction were assessed by blotting of mitochondrial and nonmitochondrial marker proteins (13, 14) (Figure 1D). The Cyto fraction was further separated into the soluble fraction (Sol) and the insoluble particulate fraction (Part), which contains plasma and organelle membranes (14) (Figure 1E). Ano1 was identified in the Mito fraction as well as the Cyto fraction and the insoluble membrane fraction obtained from the Cyto fraction (16) (Figures 1F and 1G), whereas soluble proteins, including Golgi surface-associated enzyme, FTCD (15), and cytosolic ribonucleoprotein, argonaute (Argo) 2 (17) (*see* Figure 1D), were found in the Sol fraction (Figure 1G). These results from immunohistochemical and biochemical experiments indicate the existence of Ano1 protein in the mitochondria in addition to other cellular compartments, such as the plasma membrane.

Activation of Ano1 Causes Apoptosis of RLMVECs

Cells were quiesced for 24 hours in low-serum media and then induced to proliferate with complete media. Cells were treated with Eact, a specific Ano1 activator initially identified using a drug-screen approach in an overexpressed Ano1 cell line (18). Eact activates Ano1 in a Ca^{2+}-independent manner, as described by Namkung and colleagues (18). Eact (10 μM) significantly reduced serum-induced increase in cell counts (Figure 2A). This effect was attenuated with the chloride channel

Figure 1. (Continued). (*E*) Schematic steps of mitochondria isolation. Cyto = cytosolic fraction including other non-mitochondrial membrane structures (e.g., endoplasmic reticulum, nucleus, and Golgi apparatus) and plasma membrane; Mito = mitochondrial-enriched raction; Part = insoluble (particle) proteins obtained from the Cyto fraction by ultracentrifugation; Sol = soluble fraction, obtained from the Cyto fraction by ultracentrifugation. (*F*) Representative immunoblot of whole-cell lysate (WCL), Mito fraction, and Cyto fraction from RLMVECs. To assess the purity of the Mito fraction after proteins were also blotted in addition to Ano1 (*see also E*): argonaute (Argo) 2 (cytosolic and ribosome-associated protein); Golgi 58K protein/formimino-transferase cyclodeaminase (FTCD; an enzyme associated with the cytoplasmic surface of the Golgi apparatus); sarco/endoplasmic reticulum Ca^{2+}-ATPase (SERCA; sarco/endoplasmic reticulum protein); VE-cadherin (plasma membrane protein); and histone H2A (nucleus protein). Voltage-dependent anion channel (VDAC; outer mitochondrial membrane protein); OPA1 (a protein located at the intermembrane space and inner mitochondrial membrane [IMM]), mitochondrial calcium uniporter (MCU; IMM protein) and COX IV (mitochondrial-matrix protein) were used as markers for the Mito fraction and for confirming the maintenance of mitochondrial structure integrity during the protein fractionation. Equal protein amounts of WCL, Cyto, and Mito fractions (30 μg/well) were separated by SDS-PAGE. (*G*) Representative immunoblot of Sol and insoluble Part (insoluble) proteins obtained from the Cyto fraction by ultracentrifugation (20 μg/well; *see E* and METHODS in the data supplement). WCL, the Mito fraction, and the Cyto fraction (30 μg/well) were also blotted for comparison.
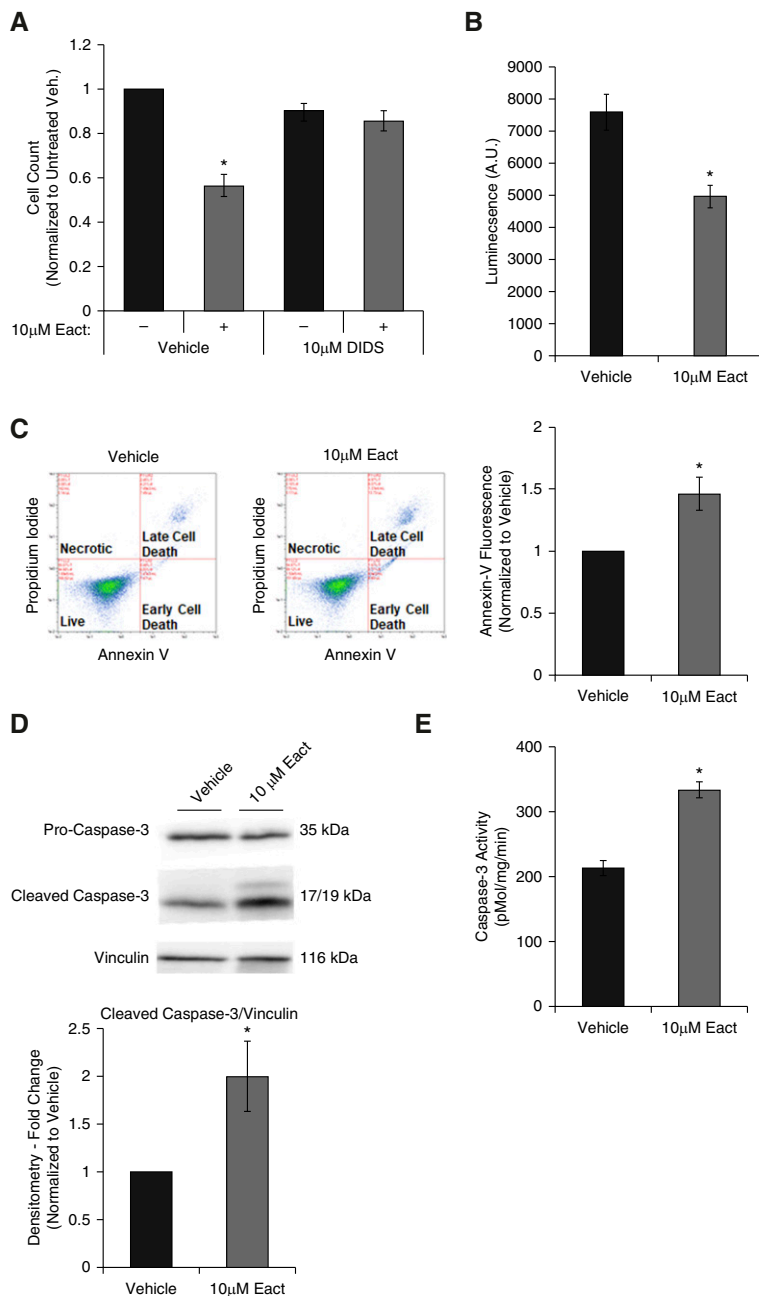
Figure 2. Activation of Ano1 induces apoptosis in RLMVECs. RLMVECs were seeded subconfluently and allowed to adhere for 24 hours before quiescing for 24 hours. Cells were then treated with drugs as indicated for 24 hours in complete media. (*A*) Cells were treated with vehicle or 10 μM Eact for 24 hours in presence or absence of chloride channel inhibitor (10 μM 4,4′-diisothiocyano-2,2′-stilbenedisulfonic acid [DIDS]; $n = 4$, two-way ANOVA with Tukey multiple comparison, *$P < 0.05$ vs. untreated control). (*B*) Cells were treated with vehicle or 10 μM Eact for 24 hours and cell viability was determined by luminescence viability assay (CellTiter-Glo; $n = 5$, *$P < 0.05$). (*C*) Cells were treated with vehicle or 10 μM Eact for 24 hours and stained for annexin-V and with propidium iodide and assessed using flow cytometry. The left two panels show representative dot plots of cells with different intensity of annexin-V and propidium iodide fluorescence. The right panel shows percent of cells positive for annexin-V fluorescence normalized to vehicle ($n = 6$, *$P < 0.05$). (*D*) Immunoblot of cleaved caspase-3 from RLMVECs treated with vehicle or 10 μM Eact ($n = 5$, *$P < 0.05$). (*E*) Caspase-3 activity from RLMVECs treated with vehicle or 10 μM Eact was measured using N-Acetyl-Asp-Glu-Val-Asp-7-amido-4-methylcoumarin fluorogenic assay ($n = 5$, *$P < 0.05$). Data are presented as mean (±SEM). A.U. = arbitrary units; veh. = vehicle.

inhibitor, 4,4′-diisothiocyano-2,2′-stilbenedisulfonic acid (DIDS) (10 μM; Figure 2A). Treatment of RLMVECs with 10 μM Eact also decreased cell viability, as assessed by CellTiter-Glo assay (Promega; Figure 2B). The reduction in cell number and viability with Ano1 activation was also associated with increased annexin-V–positive cells, as assessed by flow cytometry (Figure 2C). Immunoblot analysis demonstrated an increase in caspase-3 cleavage (Figure 2D) and an increase in caspases-3 activity (Figure 2E). Activation of Ano1 did not result in any changes in the cell cycle, as assessed by flow cytometry (Figure E3).

To confirm if the effects of Eact were specifically mediated by Ano1, siRNA was used to suppress Ano1 expression. RLMVECs transfected with Ano1-specific siRNA resulted in a significant reduction of Ano1 compared with cells transfected with scrambled siRNA (Figure 3A). Suppression of Ano1 expression attenuated caspase-3 cleavage (Figure 3B) and Eact-mediated decrease in cell number (Figure 3C) when compared with scrambled siRNA–transfected cells. Notably, we did not observe any significant difference in cell number or caspase-3 cleavage between untreated scrambled and Ano1 siRNA-transfected cells (Figures 3B and 3C).

Ano1 Activation Increases p38–Mitogen-activated Protein Kinase Phosphorylation through Mitochondrial Reactive Oxygen Species

p38–mitogen-activated protein kinase (MAPK) is an important regulator of apoptosis that is activated upon phosphorylation often in response to cell stress and reactive oxygen species (ROS). Therefore, we measured changes in p38-MAPK phosphorylation (threonine 180/tyrosine 182) after Ano1 activation. p38-MAPK activation was significantly and reproducibly increased 30 minutes after Eact administration (Figure 4A). Pretreatment with the chloride channel inhibitor, DIDS, attenuated Eact-induced p38 phosphorylation (Figure 4B). Because p38 can be activated in response to increases in mitochondrial ROS (mtROS), we pretreated cells with 1 μM (2-[2,2,6,6-tetramethylpiperidin-1-oxyl-4-ylamino]-2-oxoethyl)triphenylphosphonium chloride (Mito-TEMPO), a mitochondrial targeted ROS scavenger, before Ano1 activation.
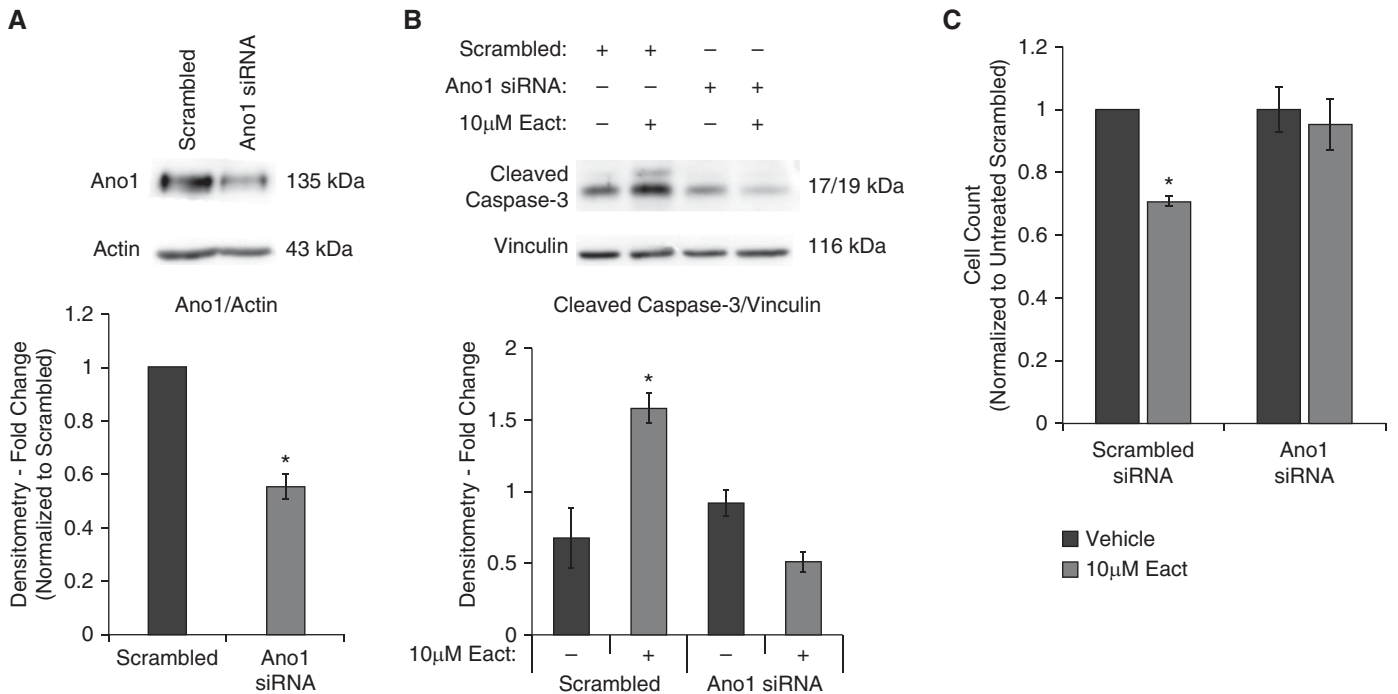
Figure 3. Eact mediates its apoptotic effects via Ano1. (*A*) RLMVECs were transfected with either scrambled or Ano1-targeted siRNA, and Ano1 expression was assessed using immunoblot (*n* = 3, *P* < 0.05). (*B*) RLMVECs were transfected with scrambled or Ano1 targeted siRNA and then treated with vehicle or 10 μM Eact for 24 hours. Expression of cleaved caspase-3 and vinculin (loading control) was then evaluated by immunoblot (*n* = 3, ANOVA with Tukey multiple comparison, *P* < 0.05). (*C*) RLMVECs were transfected with scrambled or Ano1-targeted siRNA, and cells were counted after treatment with vehicle or 10 μM Eact for 24 hours (*n* = 3, ANOVA with Tukey multiple comparison, *P* < 0.05). Data are presented as mean (±SEM).

MitoTEMPO blocked Eact-induced p38 phosphorylation (Figure 4B).

To confirm if Eact mediated p38-MAPK phosphorylation is required for cell death, we pretreated cells with 100 nM SB203580, a p38 inhibitor, or infected cells with a p38 dominant-negative construct. Overexpression of dominant-negative p38-MAPK attenuated caspase-3 cleavage in response to Ano1 activation (Figure 4C). Similarly, inhibition of p38-MAPK phosphorylation with SB203580 attenuated the Eact-mediated decrease in cell number (Figure 4D).

Ano1 Activation Alters Mitochondrial Function
Because Ano1 localized to the mitochondria and activation resulted in apoptosis, we assessed whether Ano1 activation elicited changes in mitochondrial membrane potential (ΔΨm) and mtROS levels using fluorescent plate assays to measure 5,5′,6,6′-tetrachloro-1,1′,3,3′-tetraethylbenzimidazolylcarbocyanine, iodide (JC-1) and MitoSOX fluorescence (Figures 5A and 5B). Treatment with Eact resulted in a significant loss of ΔΨm in

RLMVECs, as measured using JC-1. Eact-induced mitochondrial depolarization was attenuated by the Ano1 inhibitor, DIDS (Figure 5A). Similarly, Ano1 activation increased mtROS, as assayed using MitoSOX, a targeted mitochondrial dye that measures mitochondrial superoxide levels (Figure 5B). Pretreatment with DIDS and MitoTEMPO attenuated the increase in MitoSOX in response to Eact (Figure 5B). In addition, increased nuclear localization of Apoptosis-inducing factor, which is released from the mitochondria during apoptotic cell death, occurred in RLMVECs treated with Eact when compared with vehicle-treated cells (Figure 5C).

Ano1 Expression in PAH
We next examined if Ano1 expression was altered in PAH. We found that Ano1 expression was increased in IPAH-PAECs by immunoblot (Figure 6A). Next, we sought to determine whether activation of Ano1 would result in apoptosis of IPAH-PAECs similar to what we had observed in RLMVECs. Untreated IPAH-PAECs had a

higher cell count at 24 hours than control PAECs (Figure 6B). Treatment with 10 μM Eact markedly reduced IPAH-PAEC cell number that was attenuated in the presence of DIDS. There was a significant interaction (*P* < 0.01) with Eact treatment and IPAH status, as determined by two-way ANOVA in control and IPAH groups with and without Eact. Eact-treated IPAH cells were significantly lower than vehicle-treated IPAH cells (*P* < 0.01); however, there was a trend for Eact to decrease cell counts in control cells, but this was not significant (*P* = 0.17). In all other comparisons, there was a significant effect of IPAH, but no effect of Eact within the mitoTEMPO and DIDS treatment groups. Notably, chloride channel inhibition using DIDS did not alter cell counts of IPAH-PAECs that were not treated with Eact (Figure 6C), indicating minimal basal activity of Ano1. To confirm that Eact resulted in apoptosis in IPAH-PAECs, we examined caspase-3 cleavage. Similar to RLMVEC, Ano1 activation increased caspase-3 cleavage in IPAH-PAECs when compared with Eact-treated control ECs (Figure 6D).
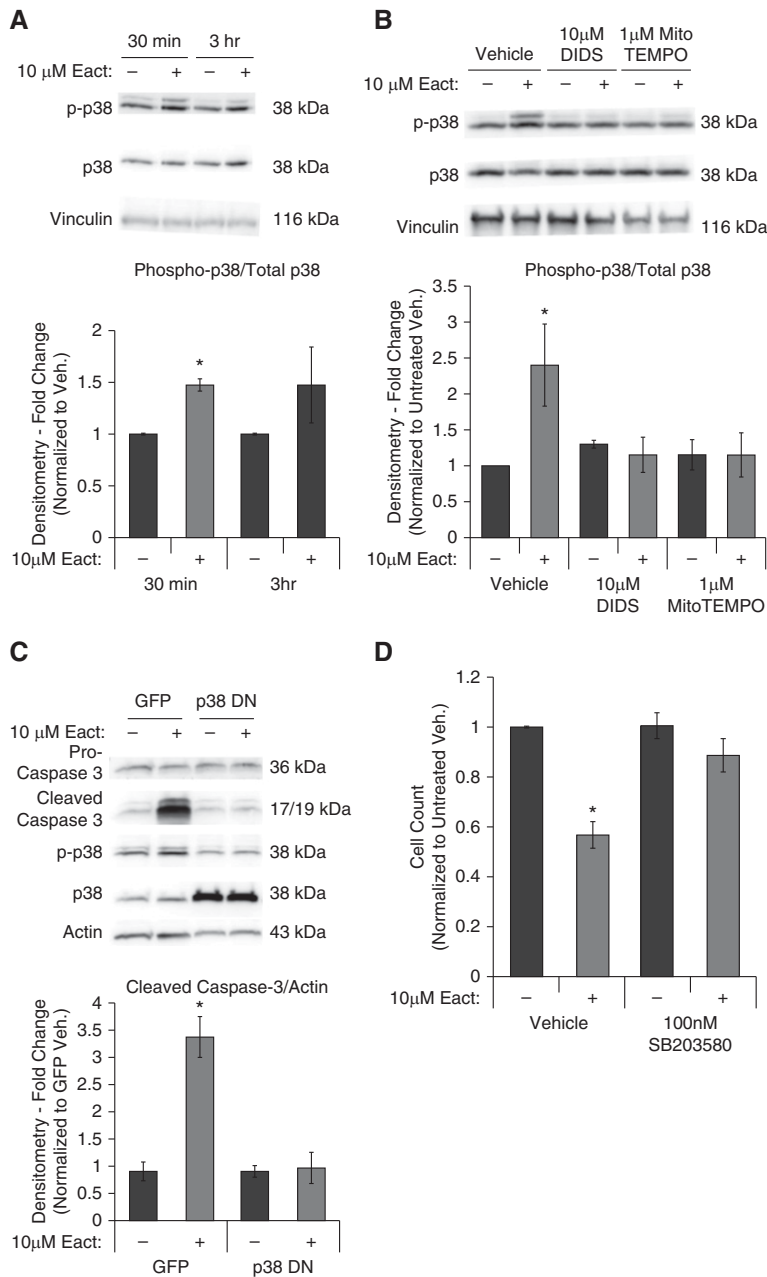
Figure 4. Ano1 activation is p38–mitogen-activated protein kinase (MAPK) dependent. RLMVECs were seeded subconfluently and allowed to adhere and infected with virus, as indicated. Cells were then quiesced for 24 hours followed by drug treatments in complete media. (*A*) p38 phosphorylation in response to Eact treatment was assessed by immunoblot at both 30-minute and 3-hour time points ($n = 5$, ANOVA with Tukey multiple comparison, *$P < 0.05$). (*B*) RLMVECs were pretreated with either 10 μM DIDS, 1 μM Mito-TEMPO, or vehicle for 1 hour and then treated with vehicle or 10 μM Eact for 30 minutes. p38 phosphorylation was then evaluated by immunoblot ($n = 5$, ANOVA with Tukey multiple comparison, *$P < 0.05$). (*C*) Cells were infected with adenoviruses containing GFP or dominant-negative p38 constructs and pro-caspase 3, cleaved caspase-3, phospho-p38, total p38, and actin expression was assessed using immunoblot ($n = 4$, ANOVA with Tukey multiple comparison, *$P < 0.05$). (*D*) Cells were treated with p38-MAPK inhibition with vehicle or 10 μM Eact in the presence/absence of SB203580 for 24 hours and cell counts were performed ($n = 4$, ANOVA with Tukey multiple comparison, *$P < 0.05$). Data are presented as mean ($\pm$SEM). Readers may view the uncut gel for Figure 4C in the data supplement. DN = dominant negative.

Hypoxia is known to increase pulmonary EC proliferation. We next examined if activation of Ano1 in a cell culture model of IPAH using hypoxic RLMVECs could counteract hypoxia-induced increases in cell number. RLMVECs were quiesced and then placed in either normoxic or hypoxic conditions for 1, 3, and 5 days in complete media. Hypoxic cells had significantly increased cell counts as compared with normoxic RLMVECs (Figure 7A). Both hypoxic and normoxic cells (3 d) treated with Eact showed comparable decreases in cell counts (significant effects of hypoxia, DIDS, and Eact, but no interaction between hypoxia and either DIDS or Eact; there was significant three-way interaction; Figure 7B). Similar to previous normoxia studies (Figure 2A), decreases in hypoxic EC counts were dependent on channel activity, as shown by DIDS (Figure 7B). Interestingly, hypoxia caused a basal increase in apoptosis, as shown by increased annexin-V (Figure 7C) and caspase-3 activity (Figure 7D), despite the overall increased cell counts. However, treatment with Eact caused a significant increase in both annexin-V and caspase-3 activity in hypoxic cells (Figures 7C and 7D).

Finally, as Ano1 expression was increased in IPAH cells, we examined if Ano1 expression was increased in hypoxic ECs, and if this expression may contribute to increased cell counts. Ano1 was moderately upregulated in response to hypoxia in RLMVECs (Figures 7E and 7F), similar to IPAH human ECs. However, siRNA (100 nM) treatment did not affect the hypoxia-induced changes in cell counts, indicating that Ano1 expression does not contribute to hypoxia-induced increases in cell number (Figure 7G).

Discussion

In this study, we demonstrate that the CaCC Ano1 is present in pulmonary EC mitochondria, and that Ano1 activation induces apoptosis by increasing mtROS-dependent p38 activation and subsequent caspase-3 activation. Furthermore, the expression of Ano1 is increased in pulmonary ECs from patients with IPAH, and activation of Ano1 results in apoptosis of ECs, which are known to be hyperproliferative, from patients with IPAH.
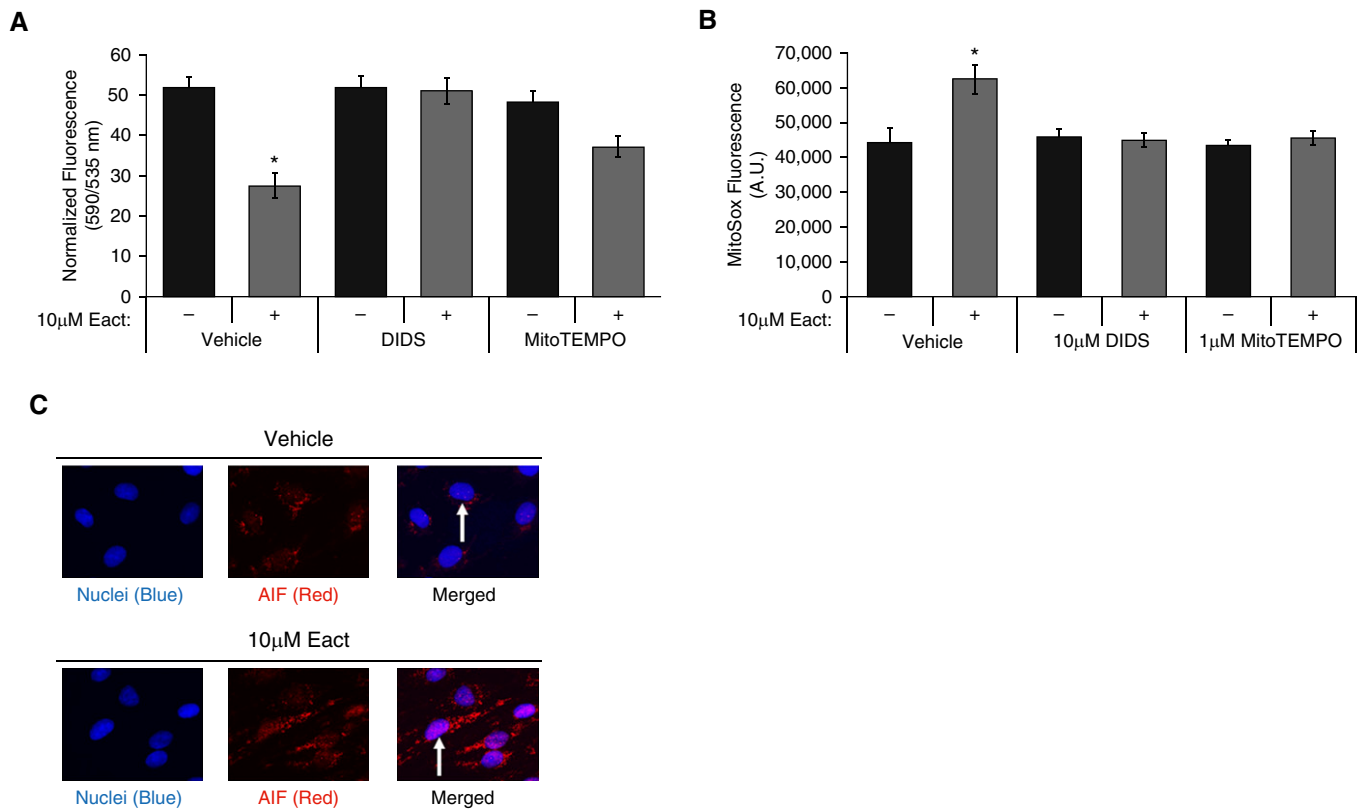
Figure 5. Ano1 activation results in loss of mitochondrial membrane potential ($\Delta\Psi$m), increased mitochondrial reactive oxygen species, and apoptosis-inducing factor (AIF) nuclear translocation. (A) RLMVECs were pretreated with 10 μM DIDS, 100 nM SB203580, 1 μM MitoTEMPO, or vehicle for 1 hour. Cells were then treated with vehicle or 10 μM Eact for 20 minutes, followed by loading with 10 μM JC-1 dye for 10 minutes before measuring 535-nm (green monomers, depolarized mitochondria) and 590-nm (red aggregate, high $\Delta\Psi$m) fluorescence. Data are presented as 590-/535-nm emission. ($n = 5$, ANOVA with Tukey multiple comparison, $P < 0.05$). (B) Cells were treated as in A and loaded with 5 μM MitoSOX for 10 minutes, followed by fluorescence measurement. ($n = 5$, ANOVA with Tukey multiple comparison, $P < 0.05$). (C) Immunofluorescence of AIF was assessed in RLMVECs treated with vehicle or 10 μM Eact for 24 hours (100$\times$). Increased Eact-induced nuclear translocation highlighted with white arrows 100$\times$, ($n = 3$). Data are presented as mean ($\pm$SEM). *$P < 0.05$ compared to vehicle control.

Although patch-clamp studies have shown CaCC currents in ECs, to the best of our knowledge, the localization of these channels in the cell has not been investigated (19). This is likely due to the fact that the molecular identity of these channels had not been confirmed until 2008 (7–9). Because Ano1 was identified as a CaCC, only one study has demonstrated Ano1 in the plasma membrane of ECs (19).

We show that the majority of Ano1 localizes to mitochondria and can affect mitochondrial function upon activation. It is known that, in addition to cation channels, the mitochondria also express anion channels, such as chloride intracellular channel 4 (CLIC4) and volume-regulated anion channel (VRAC) that can regulate mitochondrial function (20, 21). For example, increased mitochondrial CLIC4 expression and translocation has been

associated with increased p53-dependent apoptosis through dissipation of $\Delta\Psi$m (20). Our observation of depolarization of mitochondria upon activation of Ano1 would be consistent with outward Cl$^-$ current dissipating the voltage gradient across the mitochondrial inner membrane, similar to what has been observed with other mitochondrial anion channels (20).

Although small-molecule activation of Ano1 was associated with mitochondrial depolarization and apoptosis, we found that, in IPAH-PAECs, Ano1 expression was elevated. Increased Ano1 expression was also found in hypoxic ECs, but reduction of Ano1 expression with siRNA did not affect cell counts in either normoxic or hypoxic ECs. This suggests that the increase in Ano1 expression in settings of PAH is not driving a hyperproliferative phenotype in PAH ECs,

but may represent an insufficient proapoptotic compensatory response. In addition, it is likely that the increased expression of Ano1 in PAH cells may not be associated with greatly increased activity, as Eact still had a significant effect and inhibition of Ano1 alone did not alter cell number. A similar phenomenon was noted in cardiac microvascular ECs, where increased cell proliferation with hypoxia was associated with increased Ano1 expression, yet inhibition of Ano1 did not attenuate the effect of hypoxia on EC proliferation (19).

Ano1 opens in response to depolarization ($V_{1/2} = 64$ mV at 1 μM Ca^{2+}) and increased calcium (Ca^{2+} Half-maximal effective concentration [EC$_{50}$] of 5.9 μM at -100 mV) (22). Considering that the mitochondria are hyperpolarized ($\Delta\Psi$m ≈ -160 mV), it is expected that the channels would remain closed under basal
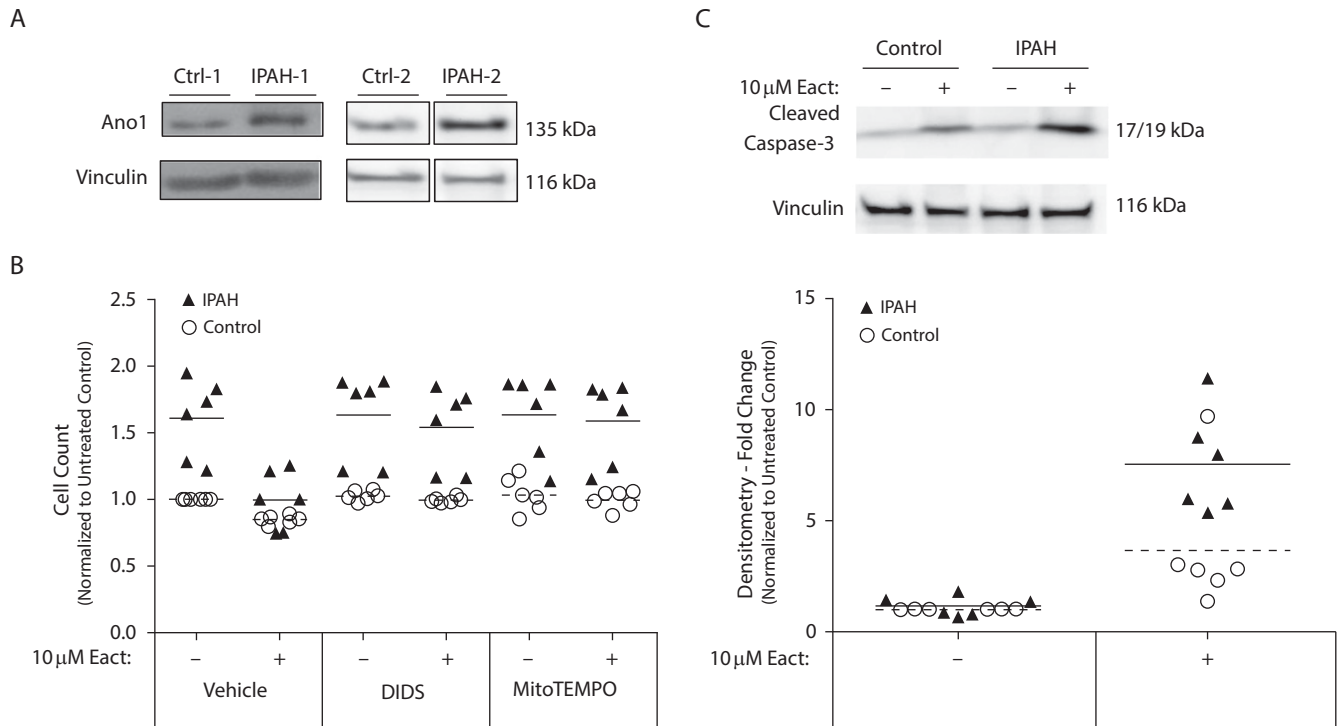
Figure 6. Ano1 activation promotes apoptosis of human idiopathic pulmonary arterial hypertension (IPAH) ECs. (*A*) Ano1 expression in isolated control and pulmonary arterial ECs from lungs of patients with IPAH assessed by immunoblot ($n = 2$). (*B*) Both control and IPAH–pulmonary artery ECs isolated from patient lungs were seeded subconfluently and quiesced for 24 hours. Cells were then pretreated as indicated for 1 hour, then treated with 10 μM Eact in serum-reduced conditions for 24 hours, after which cell counts were performed ($n = 2$ patients, triplicates). (*C*) Quiesced control and IPAH ECs isolated from patient lungs were treated with vehicle or 10 μM Eact for 24 hours, and cleaved caspase-3 expression was assessed by immunoblot ($n = 2$ patients, triplicates). Ctrl = control.

conditions. Eact activates the channel in a voltage- and calcium-independent manner, and, therefore, is able to open the channels, resulting in dissipation of negative charge in the mitochondria, resulting in depolarization. The speculation that, under basal conditions, Ano1 remains inactive is supported by our data, where cell counts and caspase-3 cleavage remain unchanged when Ano1 was molecularly suppressed in RLMVEC or inhibited by DIDS in IPAH-PAECs in the absence of Eact. It remains unclear what the precise role of mitochondrial Ano1 is for normal mitochondrial function; however, the presence of inactive Ano1 channels in the mitochondria could be leveraged as a possible proapoptotic effector in hyperproliferative cells that which have increased Ano1 expression. This is demonstrated by the enhanced effect of Eact in inducing apoptosis on IPAH-PAECs compared with control PAECs. Surprisingly, we found that RLMVEC exposed to hypoxia have enhanced apoptosis, but this does not appear to be due to increased Ano1 activity levels

associated with increased expression. This conclusion is supported by the fact that neither siRNA nor DIDS had any effect on untreated hypoxic RLMVECs. In addition, despite the increase in Ano1 expression in hypoxic ECs, there was no exaggerated effect of Eact on apoptosis and cell counts in hypoxic cells compared with normoxic cells. Hence, the effect of increased Ano1 expression *per se* in settings of hypoxia and IPAH remains unclear, and will need to be more thoroughly investigated using *in vivo* models of PH

In our studies, Ano1 activation resulted in apoptosis of pulmonary ECs. Our results are in contrast with some reports in the cancer literature, where Ano1 was identified as a positive regulator of proliferation (23). However, others have shown that Ano1 can inhibit proliferation in basilar artery smooth muscle cells or have no effect on proliferation in certain cancer cell lines (10, 11). Notably, none of these studies used activation of Ano1 to determine the effect of membrane hyperpolarization and Ca^{2+}-independent activity of Ano1 on cell fate. It is also possible that the role of Ano1 in

proliferation is dependent on cell type and underlying pathology. Further studies are needed to evaluate the underlying mechanism of the differential effects of Ano1 expression and activity in different cell lines, organelles, and conditions.

Ano1 activation was also associated with an increase in mtROS as measured by MitoSOX. Both DIDS and MitoTEMPO reduced Eact-mediated increases in mtROS. In contrast, only DIDS was capable of completely blocking the loss of $\Delta\Psi$m, whereas MitoTEMPO was not capable of attenuating the loss of $\Delta\Psi$m. Together, these observations suggest that loss of $\Delta\Psi$m in response to Ano1 activation occurs before the increase in mtROS. It has been shown that loss of $\Delta\Psi$m and increased mtROS are hallmark events that occur early in apoptosis.

Inhibition of mtROS attenuated Eact-mediated increases in p38 phosphorylation, whereas inhibition of p38 activity was not sufficient to block the loss of $\Delta\Psi$m (data not shown). This suggests that Eact-mediated increase in mtROS results in p38 activation and subsequent
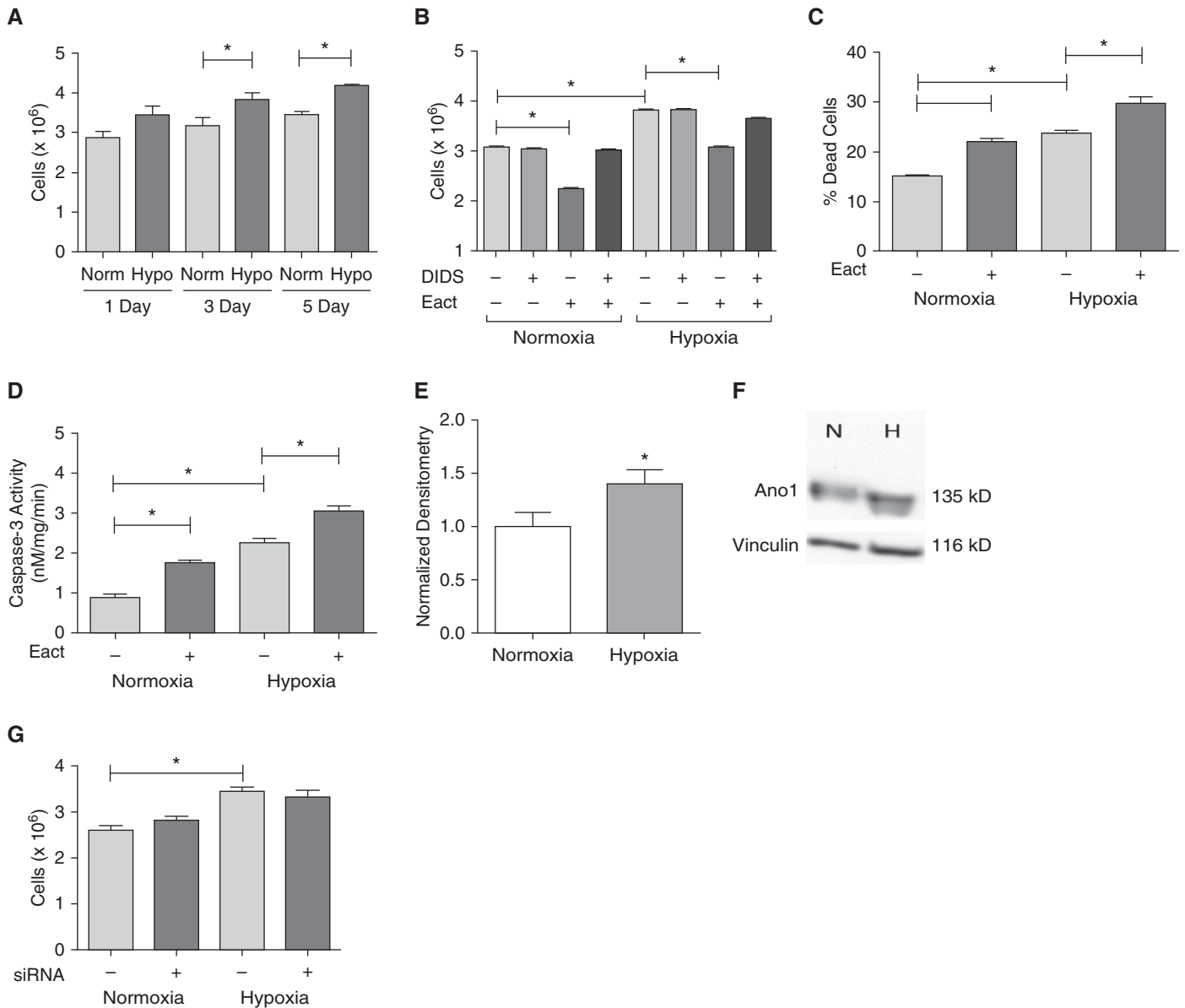
Figure 7. Hypoxia effects on RLMVECs. Cells were seeded subconfluently and then quiesced with reduced serum MCDB-131 media for 24 hours. At the start of the experiments, media were switched over to complete MCDB and cells were either exposed to normoxia (Norm) or hypoxia (Hypo) for the indicated time. (*A*) RLMVECs exposed to Hypo (1% F_{IO_2}) had higher cell counts than their normoxic counterparts (*n* = 4–6, *P < 0.05 versus Norm of time point). (*B*) RLMVECs were exposed to either normoxia or hypoxia for 3 days and pretreated with vehicle/DIDS before treatment with vehicle/10 μM Eact for an additional 24 hours, followed by cell counts (*n* = 4, *P < 0.05 using three-way ANOVA followed by Tukey *post hoc* pairwise comparison). Apoptosis in response to hypoxia and/or Eact was assessed by annexin-V staining (*C*) and caspase-3 activity (*D*) (*n* = 5, *P < 0.05, two-way ANOVA). Ano1 expression was upregulated in response to exposure to 3 days of hypoxia (*E*) (*n* = 15, *P < 0.05). (*F*) A representative blot is shown. (*G*) In another series of experiments, cells were transfected with either 100 nM scrambled or Ano1 siRNA in serum reduced media overnight. Media were then switched to complete MCDB media, and cells were placed into either normoxia or hypoxia for 24 hours and assessed by cell counts (*n* = 6, *P < 0.05, two-way ANOVA). All data are presented as mean (±SEM). Readers may view the uncut gel for Figure 7F in the data supplement.

caspase-3–mediated apoptosis. Increases in oxidant stress can trigger p38-dependent apoptosis of pulmonary ECs (24, 25). Previous studies have also demonstrated that activation of p38 is required for the induction of apoptosis downstream of mtROS (26, 27).

There are a number of limitations of the present study. First, the majority of mechanistic experiments were performed in RLMVECs, which may have considerable differences from human LMVEC. We did observe some differences in hypoxic

RLMVECs and human IPAH-PAECs, including more moderate induction of Ano1 expression in hypoxic cells compared with PAECs. Confirmation of expression and localization of Ano1 in human diseased tissue samples will also be needed to confirm

Ano1 activation as a potential therapeutic strategy. In our studies, we did not directly measure if hypoxia or IPAH cells had increased proliferation rates compared with nonhypoxic or normal human cells using specific proliferation assays. However, this has been demonstrated previously in lung ECs, and the enhanced cell counts in hypoxic cells, despite the presence of elevated apoptosis, support enhanced proliferation in this model. We believe that activation of Ano1 modifies cell number through increased apoptosis; however, a potential role in affecting proliferation rates cannot be ruled out. Finally, additional studies will be required to directly assess the role of Ano1 and efficacy of Eact in disease using appropriate *in vivo* PAH models.

In conclusion, we demonstrate, for the first time, that Ano1, a CaCC, is localized to the mitochondria of pulmonary ECs. Chemical activation of Ano1 induces apoptosis via an mtROS–p38–caspase-3 pathway. Ano1 levels are elevated in PAH, and activation in human pulmonary ECs differentially promotes apoptosis in ECs from patients with IPAH compared with control subjects. Further studies are required to determine whether Ano1 is a viable candidate for reversing the hyperproliferative phenotype associated with PAH. ∎

References

1. Guignabert C, Tu L, Girerd B, Ricard N, Huertas A, Montani D, *et al*. New molecular targets of pulmonary vascular remodeling in pulmonary arterial hypertension: importance of endothelial communication. *Chest* 2015;147:529–537.
2. Tuder RM, Groves B, Badesch DB, Voelkel NF. Exuberant endothelial cell growth and elements of inflammation are present in plexiform lesions of pulmonary hypertension. *Am J Pathol* 1994;144:275–285.
3. Tuder RM, Chacon M, Alger L, Wang J, Taraseviciene-Stewart L, Kasahara Y, *et al*. Expression of angiogenesis-related molecules in plexiform lesions in severe pulmonary hypertension: evidence for a process of disordered angiogenesis. *J Pathol* 2001;195:367–374.
4. Budhiraja R, Tuder RM, Hassoun PM. Endothelial dysfunction in pulmonary hypertension. *Circulation* 2004;109:159–165.
5. Xu W, Koeck T, Lara AR, Neumann D, DiFilippo FP, Koo M, *et al*. Alterations of cellular bioenergetics in pulmonary artery endothelial cells. *Proc Natl Acad Sci USA* 2007;104:1342–1347.
6. Masri FA, Xu W, Comhair SA, Asosingh K, Koo M, Vasanji A, *et al*. Hyperproliferative apoptosis-resistant endothelial cells in idiopathic pulmonary arterial hypertension. *Am J Physiol Lung Cell Mol Physiol* 2007;293:L548–L554.
7. Schroeder BC, Cheng T, Jan YN, Jan LY. Expression cloning of TMEM16A as a calcium-activated chloride channel subunit. *Cell* 2008;134:1019–1029.
8. Caputo A, Caci E, Ferrera L, Pedemonte N, Barsanti C, Sondo E, *et al*. TMEM16A, a membrane protein associated with calcium-dependent chloride channel activity. *Science* 2008;322:590–594.
9. Yang YD, Cho H, Koo JY, Tak MH, Cho Y, Shim W-S, *et al*. TMEM16A confers receptor-activated calcium-dependent chloride conductance. *Nature* 2008;455:1210–1215.
10. Qu Z, Yao W, Yao R, Liu X, Yu K, Hartzell C. The Ca(2+)-activated Cl(−) channel, ANO1 (TMEM16A), is a double-edged sword in cell proliferation and tumorigenesis. *Cancer Med* 2014;3:453–461.
11. Wang M, Yang H, Zheng LY, Zhang Z, Tang YB, Wang GL, *et al*. Downregulation of TMEM16A calcium-activated chloride channel contributes to cerebrovascular remodeling during hypertension by promoting basilar smooth muscle cell proliferation. *Circulation* 2012;125:697–707.
12. Comhair SAA, Xu W, Mavrakis L, Aldred MA, Asosingh K, Erzurum SC. Human primary lung endothelial cells in culture. *Am J Respir Cell Mol Biol* 2012;46:723–730.
13. O-Uchi J, Jhun BS, Hurst S, Bisetto S, Gross P, Chen M, *et al*. Overexpression of ryanodine receptor type 1 enhances mitochondrial fragmentation and Ca2+-induced ATP production in cardiac H9c2 myoblasts. *Am J Physiol Heart Circ Physiol* 2013;305:H1736–H1751.
14. O-Uchi J, Jhun BS, Xu S, Hurst S, Raffaello A, Liu X, *et al*. Adrenergic signaling regulates mitochondrial Ca^{2+} uptake through Pyk2-dependent tyrosine phosphorylation of the mitochondrial Ca^{2+} uniporter. *Antioxid Redox Signal* 2014;21:863–879.
15. Bashour AM, Bloom GS. 58K, a microtubule-binding Golgi protein, is a formiminotransferase cyclodeaminase. *J Biol Chem* 1998;273:19612–19617.
16. O-Uchi J, Sasaki H, Morimoto S, Kusakari Y, Shinji H, Obata T, *et al*. Interaction of alpha1-adrenoceptor subtypes with different G proteins induces opposite effects on cardiac L-type Ca^{2+} channel. *Circ Res* 2008;102:1378–1388.
17. Hutvagner G, Simard MJ. Argonaute proteins: key players in RNA silencing. *Nat Rev Mol Cell Biol* 2008;9:22–32.
18. Namkung W, Yao Z, Finkbeiner WE, Verkman AS. Small-molecule activators of TMEM16A, a calcium-activated chloride channel, stimulate epithelial chloride secretion and intestinal contraction. *FASEB J* 2011;25:4048–4062.
19. Wu M-M, Lou J, Song B-L, Gong Y-F, Li Y-C, Yu C-J, *et al*. Hypoxia augments the calcium-activated chloride current carried by anoctamin-1 in cardiac vascular endothelial cells of neonatal mice. *Br J Pharmacol* 2014;171:3680–3692.
20. Fernández-Salas E, Suh KS, Speransky VV, Bowers WL, Levy JM, Adams T, *et al*. mtCLIC/CLIC4, an organellular chloride channel protein, is increased by DNA damage and participates in the apoptotic response to p53. *Mol Cell Biol* 2002;22:3610–3620.
21. Tomaskova Z, Ondrias K. Mitochondrial chloride channels—what are they for? *FEBS Lett* 2010;584:2085–2092.
22. Xiao Q, Yu K, Perez-Cornejo P, Cui Y, Arreola J, Hartzell HC. Voltage- and calcium-dependent gating of TMEM16A/Ano1 chloride channels are physically coupled by the first intracellular loop. *Proc Natl Acad Sci USA* 2011;108:8891–8896.
23. Picollo A, Malvezzi M, Accardi A. TMEM16 proteins: unknown structure and confusing functions. *J Mol Biol* 2015;427:94–105.
24. Emerling BM, Platanias LC, Black E, Nebreda AR, Davis RJ, Chandel NS. Mitochondrial reactive oxygen species activation of p38 mitogen-activated protein kinase is required for hypoxia signaling. *Mol Cell Biol* 2005;25:4853–4862.
25. Grinnell K, Duong H, Newton J, Rounds S, Choudhary G, Harrington EO. Heterogeneity in apoptotic responses of microvascular endothelial cells to oxidative stress. *J Cell Physiol* 2012;227:1899–1910.
26. Amantini C, Mosca M, Nabissi M, Lucciarini R, Caprodossi S, Arcella A, *et al*. Capsaicin-induced apoptosis of glioma cells is mediated by TRPV1 vanilloid receptor and requires p38 MAPK activation. *J Neurochem* 2007;102:977–990.
27. Cuenda A, Rousseau S. p38 MAP-kinases pathway regulation, function and role in human diseases. *Biochim Biophys Acta* 2007;1773:1358–1375.